

# Wigner crystallization in quantum electron bilayers

G. Goldoni<sup>1,2</sup> and F.M. Peeters<sup>2</sup>

<sup>1</sup> *Istituto Nazionale di Fisica della Materia and Dipartimento di Fisica, Università di Modena,  
Via Campi 213/A, I-41100 Modena, Italy.*

<sup>2</sup> *Departement Natuurkunde, Universiteit Antwerpen (UIA), Universiteitsplein 1, B-2610  
Antwerpen, Belgium*

(November 22, 2018)

## Abstract

The phase diagram of quantum electron bilayers in zero magnetic field is obtained using density functional theory. For large electron densities the system is in the liquid phase, while for smaller densities the liquid may freeze (Wigner crystallization) into four different crystalline phases; the lattice symmetry and the critical density depend on the the inter-layer distance. The phase boundaries between different Wigner crystals consist of both first and second order transitions, depending on the phases involved, and join the freezing curve at three different triple points.

73.20.Dx, 64.70.Dv, 64.70.Kb

Coupled electron layers, such as those realized in semiconductor double quantum wells, are a system of current interest exhibiting a lot of new physics not present in single layers (SLs). The focus is on the peculiar properties stemming from the Coulomb interaction between the layers, such as the recently reported even denominator fractional quantum Hall states [1]. In this paper we are concerned with the influence of the inter-layer interaction on Wigner crystallization in electron bilayers (BLs) in zero magnetic field.

At sufficiently low densities a degenerate liquid of charges freezes into a lattice, which is called a Wigner crystal (WC), as the kinetic energy cost of the localization is more than compensated by the gain in Coulomb energy. Wigner crystallization has been investigated intensively over the past few years in SLs realized in semiconductor heterostructures; because a WC forms at low density, disorder-induced localization has been a serious competing mechanism which has prevented an unambiguous identification of this state. Normally, high magnetic fields are used to quench the kinetic energy and favour the crystallization, and a SL WC is believed to form for filling factors  $\nu < 1/5$  [2].

It has been suggested that in *bilayer* structures localization occurs at higher densities than in SLs, making this an appealing system for the investigation of the WC. The reason is that each layer acts as a polarizable background for the other, favouring the formation of an inhomogeneous phase [3]. Evidence of the formation of a BL WC in high magnetic fields has been found recently [4] at larger filling factors ( $\nu < 1/4$  per layer) than in SLs. On the other hand, in contrast to the SL WC, where the triangular lattice has the lowest energy [5], the BL WC might have several different lattice structures, as a result of the competition between inter- and intra-layer interactions, leading to a complex phase diagram [6–8]. A minimization of the classical potential energy [7] shows that five different crystal lattices are favoured in different ranges of inter-layer distance  $d$  and charge density  $n$ . In the classical regime the static energy and, therefore, the stable structure depends on the dimensionless product  $d\sqrt{n}$ ; in contrast, in the quantum regime the situation is more complicated as, due to the kinetic energy contribution,  $d$  and  $n$  do not scale out.

A comprehensive picture of the phase diagram of the BL WC is still lacking. The

quantum Hall regime was investigated recently within the Hartree [8] and the Hartree-Fock approximation [9] as a function of the filling factor, the layer separation, and the inter-layer tunneling. In the quantum Hall regime several solid phases have been identified which are analogous to the classical ones [7], as it is expected from the fact that the high magnetic field quenches the kinetic energy and leads the system towards the classical regime. However, the question whether all phases survive quantum fluctuations could not be addressed. Indications of the freezing transition in zero magnetic field was found within a linear response theory [3], but no information on the stable lattice structure in the different ranges of  $d$  and  $n$  was obtained.

In this paper we calculate the phase diagram of two coupled electron layers in zero magnetic field by density functional theory (DFT) [10]. The successful application of DFT to the freezing transition in several systems makes this method appealing, in view of its formal simplicity and the possibility to include accurately [within the local density approximation (LDA) [10]] exchange and correlation contributions to the energy, once these have been calculated (e.g., from simulations) for the liquid phase. DFT allows us to study both homogeneous and inhomogeneous phases on equal footing, and, therefore, to identify both solid/liquid and solid/solid phase boundaries. The system is modelled by two layers of mobile electrons with the same average density [11], compensated by a fixed uniform background of positive charge. Our results can be summarized as follows: we find that four different crystalline phases can freeze from the liquid, depending on  $d$  and  $n$ . Below the freezing density, structural transitions between the different lattices occur, the transition being of the first or second order, depending on the phases involved. Three triple points separate the liquid and the solid phases.

To set up a DFT, one has first to identify a functional of the one-particle charge density  $\rho(\mathbf{r})$  which is a good approximation of the exact free energy of the many-body system of interest which, of course, is in general unknown [12]. Recently, a functional was proposed for electrons in a SL [13] which, in terms of the plasma parameter  $r_s = (\sqrt{\pi n} a_B)^{-1}$  ( $a_B$  is the Bohr radius) predicts freezing at  $r_s \sim 32$ , in good agreement with the value  $r_s = 37 \pm 5$

obtained from simulations [14]. This approach [13] proceeds by writing the density matrix  $\rho(\mathbf{r}, \mathbf{r}')$  in terms of the single-particle density  $\rho(\mathbf{r})$  with the *ansatz*

$$\rho(\mathbf{r}, \mathbf{r}') = f(\mathbf{r}, \mathbf{r}') [\rho(\mathbf{r})\rho(\mathbf{r}')]^{1/2}. \quad (1)$$

The function  $f(\mathbf{r}, \mathbf{r}')$  can be calculated exactly for the non-interacting electron liquid,  $f(\mathbf{r}, \mathbf{r}') = 2J_1(k_F|\mathbf{r} - \mathbf{r}'|)/k_F|\mathbf{r} - \mathbf{r}'|$ , where  $J_1(x)$  is the Bessel function of the first kind and  $k_F = (2\pi\rho_0)^{1/2}$  is the 2D Fermi wavevector, with  $\rho_0$  the electron liquid density. Then one writes the kinetic energy  $E_k$ , and the exchange energy  $E_x$  (units of energy are Rydbergs)

$$E_k = - \int d\mathbf{r} \nabla_{\mathbf{r}} \nabla_{\mathbf{r}'} \rho(\mathbf{r}, \mathbf{r}')|_{\mathbf{r}=\mathbf{r}'}, \quad E_x = -(1/2) \int d\mathbf{r} \int d\mathbf{r}' |\mathbf{r} - \mathbf{r}'|^{-1} |\rho(\mathbf{r}, \mathbf{r}')|^2, \quad (2)$$

in the LDA by defining a *local* Fermi wavevector  $k_F(\mathbf{r}) = (2\pi\rho(\mathbf{r}))^{1/2}$ . Inserting (1) in  $E_k$  and  $E_x$  one obtains the total energy of a SL [15] with a (in general inhomogeneous) charge density  $\rho(\mathbf{r})$

$$E_0[\rho] = \pi \int d\mathbf{r} [\rho(\mathbf{r})]^2 + (1/4) \int d\mathbf{r} \rho(\mathbf{r})^{-1} |\nabla_{\mathbf{r}} \rho(\mathbf{r})|^2 + \int d\mathbf{r}' \int d\mathbf{r} |\mathbf{r} - \mathbf{r}'|^{-1} [\rho(\mathbf{r}) - \rho_0] [\rho(\mathbf{r}') - \rho_0] \\ - (2/3) \sqrt{2/\pi} \int d\mathbf{r} [\rho(\mathbf{r})]^{3/2} + \int d\mathbf{r} \rho(\mathbf{r}) \epsilon_c(\rho(\mathbf{r})). \quad (3)$$

The first two terms stem from  $E_k$ , the third term is the direct intra-layer Coulomb interaction, with  $\rho_0$  the average charge density, and the last two terms are the exchange and correlation contributions, respectively. In the correlation term, defined as the difference between the total energy and the kinetic and Coulomb contributions,  $\epsilon_c(\rho)$  is the correlation energy of a uniform liquid of density  $\rho$  obtained from quantum Monte Carlo calculations [14].

The above functional was very successful in predicting the freezing transition in a SL WC [13]. It is tempting to extend this theory to investigate multi-layered structures. Ideally, one would like to include the correlation energy for the complete structure, which is difficult to calculate [16]. For typical structures, however, intra-layer correlations are much more important than inter-layer correlations [17]; the latter, therefore, can be neglected in a first approximation. We write the energy functional of the bilayer system as  $E_b[\rho] = E_0[\rho] + E_I[\rho]$ , where

$$E_I[\rho(\mathbf{r})] = \int d\mathbf{r}' \int d\mathbf{r} \left[ |\mathbf{r} - \mathbf{r}'|^2 + d^2 \right]^{-1/2} \left[ \rho^A(\mathbf{r}) - \rho_0 \right] \left[ \rho^B(\mathbf{r}') - \rho_0 \right], \quad (4)$$

is the inter-layer Coulomb interaction, and the superscripts A and B label the charge densities of the two layers.  $E_b[n]$  includes (within LDA) the intra-layer correlation, which mainly determines the freezing density. In writing  $E_b$  we have neglected the tunneling between the layers as well as the finite thickness of the layers, taking the charge density profile in the direction normal to the layers as a delta-function in each layer, which is a reasonable approximation for  $d/a_B > 1$ .

In DFT one usually solves the Kohn-Sham equations self-consistently in order to obtain the charge density which minimizes  $E_b[\rho]$ . A simpler alternative (from the computational point of view) is to guess a functional form for  $\rho(\mathbf{r})$  with one or more variational parameters. Therefore, we model the charge density of the electron solid as a sum of gaussian distributions [18] centered at the lattice sites  $\mathbf{R}$ , generated by the primitive vectors  $\mathbf{a}_1$ ,  $\mathbf{a}_2$ , in one layer,  $\rho^A(\mathbf{r}) = (\alpha/\pi) \sum_{\mathbf{R}} \exp(-\alpha|\mathbf{r} - \mathbf{R}|^2)$ , and at  $\mathbf{R} + \mathbf{c}$  in the opposite layer,  $\rho^B(\mathbf{r}) = (\alpha/\pi) \sum_{\mathbf{R}} \exp(-\alpha|\mathbf{r} - \mathbf{R} - \mathbf{c}|^2)$ . To minimize the Coulomb energy,  $c$  is such that each site in one layer sits in the centre of a cell in the opposite layer.  $\alpha$  is the localization parameter; it is zero in the liquid phase and non-zero for inhomogeneous phases, and, for like densities, it is the same in both layers.

We have minimized the energy  $E_b[\rho]$  with respect to the localization parameter  $\alpha$  and to the lattice structure for fixed density and inter-layer distance [19]. Of the several possible lattices, those listed in Table I are stable in different ranges of  $d/a_B$  and  $n$ . The resulting phase diagram is summarized in Fig. 1. First, we focus on the freezing transition. For large  $d$ , i.e., weak inter-layer coupling, the freezing density tends to the single layer result  $r_s \sim 32$ . In this limit, the BL WC consists of two nearly uncoupled triangular lattices. The two lattices are staggered to minimize the residual long-range Coulomb interaction (phase D). With decreasing  $d$  the formation of an inhomogeneous phase is favoured by a gain in the inter-layer interaction and, accordingly, freezing takes place at larger densities, i.e., smaller  $r_s$ . If  $d/a_B \lesssim 32$ , inter-layer interactions become more important and the liquid freezes into

a lattice with a larger coordination number relative to sites sitting in opposite layers, namely two staggered squares (phase B) or rhombic (phase C) lattices. Along the freezing line of phase C, the angle  $\theta = \arccos \hat{\mathbf{a}}_1 \cdot \hat{\mathbf{a}}_2$  grows continuously up to  $90^\circ$  with decreasing  $d$ . For  $d/a_B \lesssim 9$ , the phase which freezes from the liquid is phase A. It consists of two staggered, rectangular lattices; the aspect ratio  $\beta = |\mathbf{a}_2|/|\mathbf{a}_1|$  at freezing is larger than 1 and its value depends on  $d$ . For  $\beta = 1$ , phases A and B coincide.

When  $n$  is swept through the freezing density,  $n_f$ , the value of the localization parameter  $\alpha$  at which the energy minimum is attained leaps from zero (for  $n > n_f$ ) to a finite value (for  $n < n_f$ ) such that  $\alpha r_s^2 \sim 0.6$ . This corresponds to a very delocalized charge density so that the Lindemann's ratio  $\gamma$ , defined as the root mean square fluctuation around a lattice site divided by the lattice parameter, coincides in practice to its upper limit [20], corresponding to a uniform density, which is, e.g.,  $\gamma = 0.373$  for phase D, and  $\gamma = 0.408$  for phase B.

In Fig. 1 the open circles are the results of Świerkowski *et al.* [3], who found a singularity in the linear response function of the BL electron liquid. These points correspond very well with our calculated BL WC freezing boundary. In Ref. [3] the symmetry of the lattice which freezes from the liquid was not identified, but the wavevector at which the singularity occurs is  $q/k_F \simeq 2.5$ . Since  $q/k_F = 2.50$  for phase B, while  $q/k_F = 2.69$  for phase D, it seems that the inhomogeneous phase found in Ref. [3] is in fact phase B, again in agreement with our calculation.

We next consider transitions between the different solid phases. As seen above, lowering  $n$  at large  $d$  freezes the liquid into phase D. If the density is further decreased, i.e.,  $r_s$  is increased at fixed  $d$ , the intra-layer interaction weakens with respect to the inter-layer interaction. This lowers the energy of phase C which finally becomes energetically favoured. Since phases C and D belong to different symmetry classes this is a first order phase transition [6]. In the region of phase C, the energy minimum is at  $\theta \neq 90^\circ$ , while  $\theta = 90^\circ$  corresponds to a maximum; on reducing  $n$  or  $d$ , the energy minimum moves towards  $\theta = 90^\circ$ , which finally becomes a minimum and the lattice makes a continuous transition to phase B. Another structural phase transition occurs between phases A and B, at sufficiently low density,

when  $d/a_B \gtrsim 9$ . The transition is a continuous one, where the aspect ratio becomes larger than 1 at a critical density, which depends on  $d$ . An example of the overall evolution of the aspect ratio is shown in Fig. 2 for  $d/a_B = 14$ ;  $\beta$  first reaches a maximum and then decreases. When  $r_s \gg d/a_B$ , however, the present calculation becomes less accurate as inter-layer correlations beyond the static Coulomb interaction, which are not important near the freezing transition [17] and which were neglected here, become more important. Finally, the A/B, B/C and C/D transition curves join the freezing curve at three triple points where the solid phases and the liquid have the same energy.

To conclude, we note that, as an alternative to high magnetic fields, one can use particles with a small effective Bohr radius, like electrons in silicon layers [21] or holes [22], to quench the kinetic energy. The range of densities for the BL WC in zero magnetic field should be within reach in coupled layers of holes grown along high index crystallographic directions [23], where both high effective masses, to quench the kinetic energy, and high mobilities, to prevent defect-induced localization, can be obtained.

We acknowledge financial support from the HCM network No. ERBCHRXCT930374, a NATO Collaborative Research Grant, and the Belgian National Science Foundation. One of us (FMP) acknowledges discussions with M. Das during the initial stage of this work and the hospitality of the Australian National University (Canberra). We are grateful to G. Senatore for enlightening discussions.

## REFERENCES

- [1] Y.W. Suen *et al.*, Phys. Rev. Lett. **68**, 1379 (1992); J.P. Eisenstein *et al.*, *ibid.* **68**, 1383 (1992).
- [2] V.J. Goldman *et al.*, Phys. Rev. Lett. **65**, 2189 (1990); V.J. Goldman *et al.*, *ibid.* **70**, 647 (1993).
- [3] L. Świerkowski, D. Neilson, and J. Szymański, Phys. Rev. Lett. **67**, 240 (1991).
- [4] H.C. Manoharan, Y.W. Suen, M.B. Santos, and M. Shayegan, Phys. Rev. Lett. **77**, 1813 (1996).
- [5] L. Bonsall and A.A. Maradudin, Phys. Rev. B **15**, 1959 (1977).
- [6] V.I. Falko, Phys. Rev. B **49**, 7774 (1994); K. Esfarjani and Y. Kawazoe, J. Phys.: Condens. Matter **7**, 7217 (1995).
- [7] G. Goldoni and F.M. Peeters, Phys. Rev. B **53**, 4591 (1996); G. Goldoni, V.A. Schweigert, and F.M. Peeters, Surf. Sci. **361/362**, 163 (1996).
- [8] S. Narasimhan and T.-L. Ho, Phys. Rev. B **52**, 12291 (1995).
- [9] L. Zheng and H.A. Fertig, Phys. Rev. B **52**, 12282 (1995).
- [10] See, e.g., *Theory of the Inhomogeneous Electron Gas*, edited by S. Lundqvist and N. H. March (Plenum Press, New York, 1983).
- [11] Layers of like densities are realized by gate tuning as to preserve symmetric charge distribution [1].
- [12] See Ref. [18] for the three-dimensional electron gas and A.R. Denton *et al.*, Phys. Rev. Lett. **64**, 1529 (1990) for the hard sphere liquid.
- [13] N. Choudhury and S.K. Ghosh, Phys. Rev. B **51**, 2588 (1995).
- [14] B. Tanatar and D.M. Ceperley, Phys. Rev. B **39**, 5005 (1989).



- [15] In semiconductor accumulation layers the positive background sits in a layer at a distance  $d_b$  from the electron layer. This shifts the energy of the system by a constant  $2\pi ne^2/d_b$ , corresponding to the electrostatic energy of a plane capacitor. As we are only interested in energy differences, this contribution has been neglected.
- [16] For BLs, there exists no analogue for the correlation expression which was obtained with quantum simulations [14] for SLs. An approximate calculation of inter-layer correlations in the liquid phase was worked out within the Singwi-Tosi-Land-Sjölander approach in Ref. [17] and in L. Zheng and A.H. MacDonald, **49**, 5522 (1994).
- [17] J. Szymański, L. Świerkowski, and D. Neilson, Phys. Rev. B **50**, 11002 (1994).
- [18] G. Senatore and G. Pastore, Phys. Rev. Lett. **64**, 303 (1990).
- [19] The integrals in the first term in (3) and in the potential energy terms [third term in (3) and (4)] were conveniently performed in reciprocal space by Fourier-transforming  $\rho(\mathbf{r})$ , while the remaining integrals were performed in real space. Typically, six shells both in direct and reciprocal lattices were used in the calculations.
- [20] C.N. Likos, S. Moroni, and G. Senatore, Phys. Rev. B, in press.
- [21] V.M. Pudalov, M. D'Iorio, S.V. Kravchenko, and J.W. Campbell, Phys. Rev. Lett. **70**, 1866 (1993).
- [22] S. Shapira *et al.*, Surf. Sci. **361/362**, 113 (1996).
- [23] M. Henini *et al.*, Appl. Phys. Lett. **65**, 2054 (1994); S. Hill *et al.*, Physica B **211**, 440 (1995).

## FIGURES

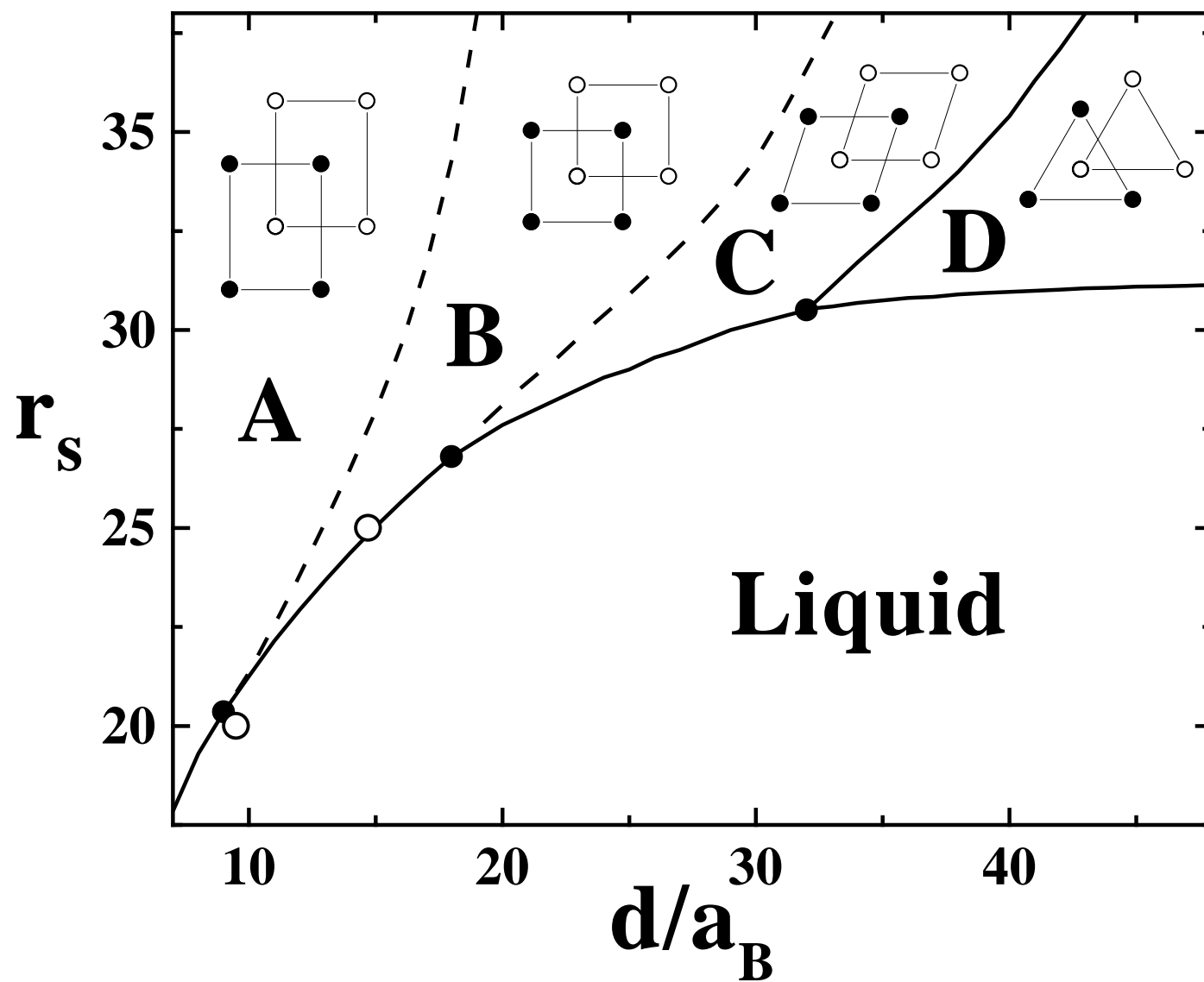
FIG. 1. Phase diagram of the electron bilayer. Solid curves: first order phase transitions. Dashed curves: continuous phase transitions. Solid dots: triple points. Open dots: freezing transition deduced from Ref. [3].

FIG. 2. Evolution of the aspect ratio  $\beta$  for phase A at  $d/a_B = 14$  obtained by minimization of  $E_b[n]$  with respect to  $\beta$  and  $\alpha$ .

# TABLES

TABLE I. Lattice parameters of phases A, B, C and D.  $a$  is the nearest-neighbour distance. For each phase, the primitive vectors  $\mathbf{a}_1$  and  $\mathbf{a}_2$ , the inter-lattice displacement  $\mathbf{c}$ , the reciprocal lattice vectors  $\mathbf{b}_1$  and  $\mathbf{b}_2$ , and the charge density  $n_s$  are indicated.  $\beta = |\mathbf{a}_2|/|\mathbf{a}_1|$  and  $\theta$  is the angle between  $\mathbf{a}_1$  and  $\mathbf{a}_2$ .

Phase	$\mathbf{a}_1/a$	$\mathbf{a}_2/a$	$\mathbf{c}$	$\mathbf{b}_1/(2\pi/a)$	$\mathbf{b}_2/(2\pi/a)$	$n_s a^2$
A (Staggered rectangular)	$(1, 0)$	$(0, \beta)$	$(\mathbf{a}_1 + \mathbf{a}_2)/2$	$(1, 0)$	$(0, 1/\beta)$	$1/\beta$
B (Staggered square)	$(1, 0)$	$(0, 1)$	$(\mathbf{a}_1 + \mathbf{a}_2)/2$	$(1, 0)$	$(0, 1)$	1
C (Staggered rhombic)	$(1, 0)$	$(\cos \theta, \sin \theta)$	$(\mathbf{a}_1 + \mathbf{a}_2)/2$	$(1, -\cot \theta)$	$(0, \sin^{-1} \theta)$	$\sin^{-1} \theta$
D (Staggered triangular)	$(1, 0)$	$(1/2, \sqrt{3}/2)$	$(\mathbf{a}_1 + \mathbf{a}_2)/3$	$(1, -1/\sqrt{3})$	$(0, 2/\sqrt{3})$	$2/\sqrt{3}$



G.Goldoni et al. - Fig. 2

